

Structure Analysis of Zinc Oxide Nanorods Synthesized by Cost Effective Precipitation Method Applicable for UV Protection

AP Sunitha^{1*}, K Nayana² and NE Unnimaya³

¹Department of Physics, Government Victoria College, Kerala, India

²Department of Physics, NSS College, Kerala, India

³Department of Physics, Sree Vivekananda PadanaKendram Arts and Science College, Kerala, India

*Corresponding author: AP Sunitha, Department of Physics, Government Victoria College, Kerala, India.

E-mail: sunithaganesh@gvc.ac.in

Received: May 19, 2021; Accepted: June 2, 2021; Published: June 9, 2021

Abstract

Zinc Oxide (ZnO) has very attractive properties among nanomaterials with wide verity of applications. In this article simple and cost effective synthesis and detailed structure analysis of nanorods of ZnO prepared by chemical precipitation method at room temperature is reported. Powder of as synthesized ZnO nanorods are characterized by XRD, absorption spectra, dynamic light scattering (DLS), TEM and SAED. The XRD pattern shows the wurtzite crystal structure with average crystalline size as 29 nm by Debye-Scherrer formula and 24.5 nm by Williamson-Hall (W. H) plot. W. H plot also give a strain of -0.0004. From XRD, dislocation energies, lattice constants, d space are also tabulated. Broad peak in absorption spectra in ultra violet range indicate that the nanorods are applicable in textiles, sun creams and UV protection windows, industries as an ultraviolet absorber. Ultra violet radiation is very hazardous to human body. So, materials, especially nanomaterials with large surface to volume ratio and ultra violet absorption property have got a lot of acceptance. TEM characterizations also prove the nanorod structure with diameter of the order of 50 nm and length greater than 200 nm. DLS experiment estimated the size of synthesized structure. Selected area electron diffraction (SAED) pattern verifies the polycrystalline nature of ZnO nanorods and got an interplanar distance of 0.26 nm.

Keywords: Zinc oxide nanorods; Precipitation; Dynamic Light Scattering (DLS)

Introduction

Among II-VI group compounds, zinc oxide (ZnO) is very popular with large number of applications [1-3]. In bulk form, it possesses a wide direct bandgap of 3.3 eV [4-6]. In nanof orm, the bandgap can be varied by varying the size of nanoparticle. The bandgap engineering property of nanostructures makes them possible to use in verity of applications [2]. Properties of nanostructures of ZnO can be tuned by changing its morphology and size [7-8]. Most common structure of ZnO is hexagonal wurtzite with lattice constants a and b equal to 3.2495 Å and c equals 5.2062 Å [9-10]. The ratio of c/a is 1.6. Wurtzite structure has no center of symmetry [11]. Hexagonal close packed zinc and oxygen lattices intertwined to form wurtzite structure [2]. Both zinc and oxygen ion has a coordination number of 4. Sp³ hybridized crystals generally show n-type conductivity [2,12].

ZnO has been recognized as pigment in paintings from earlier period itself. It is also applied as vulcanization accelerator in rubber industries, as chemical in ointments and in skin protectors [2,9] etc. Recently, properties like high electron mobility, stability and large specific surface area of ZnO are used in gas sensing applications [13-17]. Organic pollutants can be removed from water by making use of ZnO as photocatalyst for photodegradation [18-19]. Because of high electron mobility

of ZnO, it can be used in excitonic solar cells like hybrid [1] and dye sensitized solar cells [20] as charge transport material. Low refractive index of 2.05, and high exciton binding energy of 60 meV attracts application of ZnO to Optical devices [2]. Since the exciton binding energy is inversely proportional to the square of Bohr exciton radius, large exciton binding energy indicates the tight binding among excitons. So thermal degradation of exciton will not occur at room temperature and this will help to design UV laser and detectors at room temperature.

Among wide bandgap semiconductors with similar structure and properties, ZnO with high exciton binding energy has an advantage of room temperature excitonic transitions [7, 10, 21-24]. In piezoelectric devices, the large value of piezoelectric coupling coefficient of ZnO is very useful [25-26]. The absorption capacity in UV range and non-toxic behavior [11,27] lead to wide acceptance in cosmetics. Due to the electrochemical qualities, ZnO and its nanocomposites can also be used as electrode in supercapacitors [28-29]. Studies also show that, ZnO has antibacterial properties to resist gram positive and negative bacteria, Bacillus subtilis, e coli etc. [27-30]. In textile industry, ZnO nanoparticles act as UV light absorber [31].

ZnO nanorods synthesis can be done by various methods. Y. Tak et al prepared ZnO nanorods by thermal evaporation and solution method on silicon substrate [32]. L. Wang et al. [17], and O. Akhavan [19] synthesized nanorods by hydrothermal treatment. W.I Park et al synthesized nanorods of ZnO by electron beam evaporation method [33]. In this work, ZnO nanorods are synthesized by economically feasible and simple [7] chemical precipitation method at room temperature. Because of no need of templates or catalysts, chemical precipitation method is good among large scale production methods [6]. Zinc acetate dihydrate and sodium hydroxide are used as precursors. Polyvinyl pyrrolidone (PVP) is used as capping agent. The reaction is thermodynamically favourable with releasing of energy at the time of precipitation of ZnO [34]. A. M. Pourrahimi et al. proved that nanostructure ZnO created from Zinc acetate is more stable than zinc chloride and zinc nitrate and zinc sulphate [35]. In this article, cost effective preparation of ZnO nanorods by chemical precipitation method and structure analysis of the synthesized nanostructure by various methods like XRD, W-H plot, TEM, SAED etc is reported.

Methods

0.2 molar of zinc acetate dihydrate ($ZnC_4H_6O_4$). $2H_2O$ and 0.2 molar of sodium hydroxide (NaOH) were used as precursors. Poly vinyl pyrrolidone (PVP) was used as capping agent. All the chemicals were of analytical grade. To get 0.2 molar of zinc acetate solution, 2.2 g of it was dissolved in 50 ml deionised water. At the time of stirring in 1200 rpm, 1 g of PVP dissolved in 50 ml water was poured drop by drop to the solution. After getting a uniform solution, 0.2 molar sodium hydroxide solution was added drop by drop to the solution and it continually stirred for 3 hours at 1200 rpm to get precipitated. The whole process was carried out at room temperature. The supernatant precipitate containing nano size zinc oxide is separated and washed with water and iso propyl alcohol. The final product was dried in an air oven at 100°C for one hour.

The chemical reaction of synthesis is,



Crystal structure of as synthesised ZnO was examined by Xray diffractometer (PANalytical X'Pert PRO) with Cu-K α radiation. Wave length of radiation is 0.15406 nm and scan range was 10-90 degree, glancing angle scan. UV-Vis-NIR spectrometer (Jasco-V-570, UV/VIS) with detector resolution of 0.1 nm in UV-Visible region and 0.5 nm in NIR region was used to plot absorption spectra. Dynamic light scattering characteristics was done by (DLS, SZ-100, Horiba Scientific) for 40 ns, 80 ns and 120 ns gate delay times. Transmission electron microscopic (TEM) images were taken to analyse the nanostructure formation. SAED was taken to confirm the crystalline structure and to find the d spacing.

Results and Discussions

The XRD pattern of synthesised ZnO is shown in FIG. 1a. The distinct peaks at angles (2θ) 32.0499, 34.7190, 36.5377, 47.8596, 56.8586, 63.1269, 68.1995, 69.3278 indicate the structure of ZnO as wurtzite hexagonal structure. Corresponding crystallographic planes are (100), (002), (101), (102), (110), (103), (112), (203). It is verified using JCPDS data (card number: 36-1451) and listed in TABLE 1. Interplanar distance (d-spacing) is calculated using Bragg's diffraction equation (1). Average crystalline size (D) is determined using the Debye-Scherrer equation (2) [10,36-40]. Where β is the full width at half maximum (FWHM) of various XRD peaks. Crystalline sizes estimated are listed in TABLE 1. Crystalline size may

different from particle size. Crystalline size is the size of crystal with coherent diffraction [41].

$$2d\sin\Theta=n\lambda \tag{1}$$

$$D=K\lambda/\beta\cos\Theta \tag{2}$$

Average crystalline size and strain are calculated using Williamson-Hall method [36]. According to this method, the peak broadening in XRD is not only due to crystalline size. Strain also contributes to peak broadening. The relation for peak broadening is,

$$\beta_T=\beta_D+\beta_S \tag{3}$$

Where β_D is the crystalline size peak broadening and β_S is the strain peak broadening and β_T is the total broadening. Instrumental broadening is neglected here. Expression for crystalline and strain broadening are,

$$\beta_D=K\lambda/D\cos\Theta \tag{4}$$

$$\beta_S=4\epsilon\tan\Theta \tag{5}$$

where λ is the wavelength of radiation used in XRD (0.15406 nm), K is the particle shape dependent factor (K=0.9), ϵ is the strain and Θ is the angle of diffractions.

Putting equation (4) and (5) in (3) give,

$$\beta_T\cos\Theta=K\lambda/D+4\epsilon\sin\Theta \tag{6}$$

The plot between $4\sin\Theta$ along X axis and $\beta_T \cos\Theta$ along Y-axis using equation (6) and linear curve fitting result in y intercept as $K\lambda/D$ and slope as strain ϵ . Williamson-Hall plot is given in FIG. 1b. Y intercept of the plot is 0.00566 which result in a crystalline size of 24.50 nm and strain (slope) is -0.00047. The negative strain indicates the strain behaviour as compressive and it may be due to the shrinkage of crystals [10,42-43].

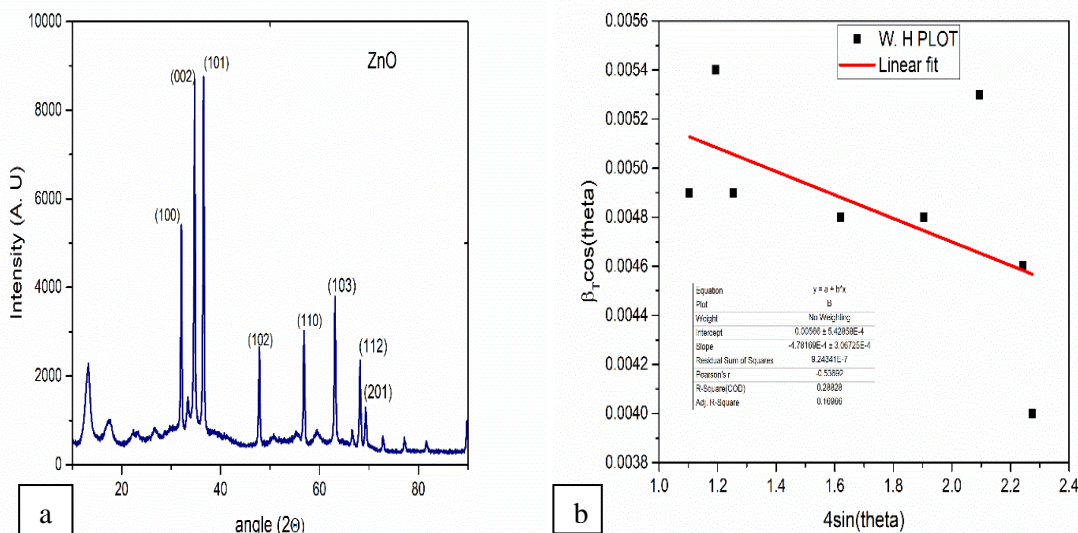


FIG. 1. (a) XRD of ZnO nanorods. (b) W.H Plot to find strain.

TABLE 1. XRD results.

XRD Peak (hkl)	2θ (observe d)	D-spacing (Observed) (Å°)	Crystalline size (D) (nm)	FWHM (β _T) (Degree)	β _T CosΘ (Radians)	4sinΘ	Crystalline size (D) (nm)	Dislocation density (Δ) x 10 ¹⁵ /m ²	Lattice constant 'a' (Å°)	Lattice constant 'c' (Å°)
100	32.0499	2.7904	28.02	0.2954	0.0049	1.1042	28.02	3.8	3.2220	-
002	34.7190	2.5816	25.68	0.3236	0.0054	1.1935	25.68	4.55	-	5.1635

101	36.5377	2.4573	28.02	0.299	0.0049	1.2539	28.02	3.8	-	-
102	47.8596	1.8990	29.20	0.2973	0.0048	1.6212	29.20	3.52	-	-
110	56.8586	1.6180	29.20	0.3092	0.0048	1.9043	29.20	3.52	3.2360	-
103	63.1269	1.4716	26.16	0.3549	0.0053	2.0938	26.16	4.38	-	-
112	68.1995	1.3740	30.14	0.3187	0.0046	2.2425	30.14	3.3	-	-
201	69.3278	1.3543	34.66	0.2773	0.0040	2.2750	34.66		-	-

For hexagonal close pack structure, lattice constants and d spacing are connected by the equation (6) [36].

$$\frac{1}{d^2} = \frac{4}{3} \left(\frac{h^2 + hk + k^2}{a^2} \right) + \frac{l^2}{c^2} \quad (6)$$

Combining equation (1) and (6),

$$\sin^2 \Theta = \lambda^2 (h^2 + hk + k^2) / 3a^2 + l^2 \lambda^2 / 4c^2 \quad (7)$$

By equation (7), crystallographic planes with $l=0$, lattice constant a is

$$A = \lambda (h^2 + hk + k^2)^{1/2} / \sqrt{3} \quad (8)$$

and crystallographic planes with $h=k=0$, lattice constant c is

$$c = l \lambda / 2 \sin \Theta \quad (9)$$

possible values of a and c calculated are listed in TABLE 1. It is in good agreement with the theoretical values.

By Williamson-Smallman's formula [44], the minimum dislocation energy can be written in terms of crystalline size D as the equation (10). Dislocation density is the total length of dislocation line per unit volume. Dislocation densities from equation (10) also listed in TABLE 1

$$\Delta = 3/D^2 \quad (10)$$

Absorption spectra of ZnO are shown in FIG. 2. A broad peak in UV range between 370 nm to 250 nm indicate the poly disperse nature of powder. It is clear that as synthesised ZnO nanorods can absorb dangerous UV radiations and can be used in textile and sun cream industries [31]. Peak of band is at 353 nm. Corresponding band gap calculated by the equation (11) is 3.499 eV. Band gap is again verified by the Tauc relation (12) and the plot is inserted in FIG. 2. For direct band gap crystals, Tauc plot is drawn between $(\alpha h\nu)^2$ and $h\nu$ [1,4,36,45]. Where α , ν and h are absorbance, frequency of radiation and Plank's constant respectively. E_b is the band gap of ZnO crystal in the bulk (3.3 eV). Tauc plot also gives a band gap of 3.31 eV. A is a constant.

$$E = hc/\lambda \quad (11)$$

$$A h\nu = A (h\nu - E_b)^{1/2} \quad (12)$$

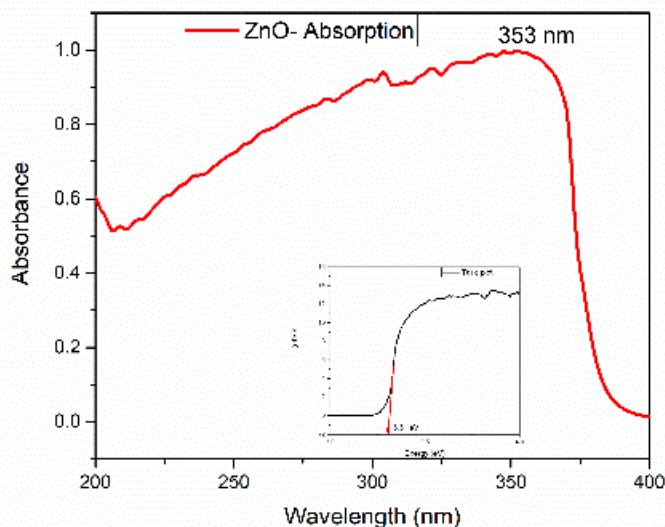


FIG. 2. Absorption spectra and Tauc plot

Dynamic light scattering (DLS) is a well-known method to find out size of nano particles. It works on the principle of Brownian motion of particle in a solution. Since the smaller particle move in fast than bigger particles, the interference pattern of scattered radiations varies with respect to the size of particles. From the interference the size of particles can be estimated. The gate delay time represents the duration of pulse of radiation incident on the solution. Changing the gate delay time determines the size of particles to be determined. Here, 40 ns, 80 ns and 120 ns are the chosen gate delay times. Calculated hydrodynamic particle size and standard deviation are plotted. FIG. 3 shows the graphs of size estimation by DLS. In FIG. 3a hydrodynamic particle size versus gate delay time and in FIG. 3b, frequency (%) of particles detected versus average diameter is plotted.

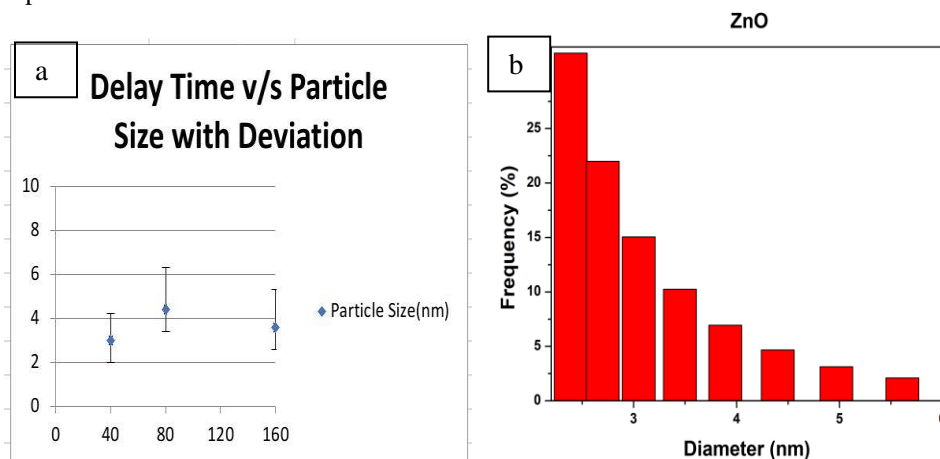


FIG 3. (a) Dynamic Light Scattering Plots at different gate delay time (b) Frequency of particles plot with average diameter as per DLS measurement for 40 ns gate delay.

Synthesized ZnO nanoparticles were further examined by Transmission electron microscopy (TEM) as shown in FIG. 4. It shows the synthesized nanostructure is purely nanorods with length greater than 200 nm and diameter below 50 nm. FIG. 4c shows the interplanar distance of 0.26 nm. Similar results are reported in the works by A. Medina et al. [6] and Y. Tak et al. [32] as the interplanar distance of ZnO nanorods. FIG. 4d is the selected area electron diffraction pattern (SAED) of ZnO nanorods. The bright spots are the clear indication of poly crystalline nature of synthesized nanorods, which agree the XRD pattern. Interplanar distance can be calculated from the SAED pattern by the relation

$$D=2/\text{distance between bright spots}=1/r \quad (13)$$

where r is the radius of circle created by bright spots in SAED pattern. Calculated interplanar distance from the diameter of 8.861 nm^{-1} in reciprocal lattice is 0.23 nm . Interplanar distance or d spacing in ZnO nanocrystals estimated from FIG. 4c and FIG. 4d are in perfect match with the same calculated from XRD.

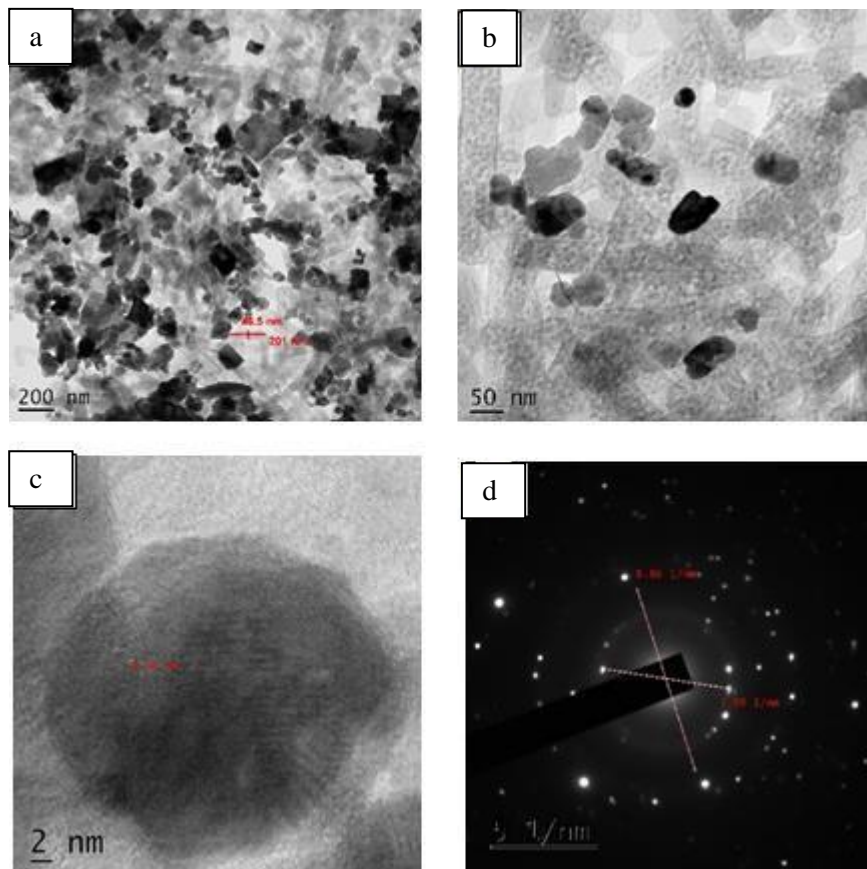


FIG. 4. (a, b, c) are TEM images in different scales. (d) SAED pattern

Conclusion

Zinc oxide nanorods synthesized by chemical precipitation method is polycrystalline in nature. XRD pattern verify that the structure of synthesized ZnO crystals is wurtzite structure of ZnO. Crystalline sizes of nanorods are found near 29 nm from XRD. Lattice constants, dislocation densities are calculated and tabulated. Interplanar distance calculated by XRD and SAED are in well agreement with each other. SEAD image shows the clear poly crystalline with bright spots. TEM images prove the nanorod structure with average diameter as 50 nm and length above 200 nm . Wide absorption spectra between 250 nm to 370 nm indicate that the as synthesized nanostructured ZnO is applicable in Ultraviolet preventing applications like sun creams, windows and textile industries.

Acknowledgement

APS acknowledges Dr. K. J. Saji, Assistant Professor in Photonics, Kochi University of Science and Technology, Kochi-22 and Dr. K. Sandeep, Department of Chemistry, Government Victoria College, Palakkad, Kerala for characterization facilities, and DST-Fist, Department of Physics, Government Victoria College, Palakkad, Kerala

Author Contribution

APS experiment, documentation, communication; KN documentation; NEU experiment

References

1. Middya S, Layek A, Dey A, et al. Morphological impact of zno nanoparticle on MEHPPV:zno based hybrid solar cell. *J Mater Sci Mater Electron*. 2013;24(11):4621-4629.
2. Borysiewicz MA. Zno as a functional material: A review. *Crystals*. 2019;9(10).
3. Jayanthi K, Chawla S, Sood KN, et al. Dopant induced morphology changes in zno nanocrystals. *Appl Surf Sci*. 2009;255(11):5869-5875.
4. M SS, Bose L, Kc G. optical properties of zno nanoparticles. 2009;16(1):57-65.
5. Wang J, Chen R, Xiang L, et al. Synthesis, properties and applications of zno nanomaterials with oxygen vacancies: A review. *Ceram Int*. 2018;44(7):7357-7377.
6. Medina A, Béjar L, Borjas SE, et al. Characterization of zno nanoparticles with short-bar shape produced by chemical precipitation. *Mater Lett*. 2012;71:81-83.
7. Khoshhesab ZM, Sarfaraz M, Asadabad MA. Preparation of zno nanostructures by chemical precipitation method. *Synth React Inorganic, Met Nano-Metal Chem*. 2011;41(7):814-819.
8. Hsieh CH. Spherical zinc oxide nano particles from zinc acetate in the precipitation method. *J Chinese Chem Soc*. 2007;54(1):31-34.
9. Prabhu YT, Rao KV, Kumar VSS, Kumari BS. Synthesis of zno Nanoparticles by a Novel Surfactant Assisted Amine Combustion Method. *Adv Nanoparticles*. 2013;02(01):45-50.
10. Mustapha S, Ndamitso MM, Abdulkareem AS, et al. Comparative study of crystallite size using Williamson-Hall and Debye-Scherrer plots for zno nanoparticles. *Adv Nat Sci Nanosci Nanotechnol*. 2019;10(4).
11. Talam S, Karumuri SR, Gunnam N. Synthesis, characterization, and spectroscopic properties of zno nanoparticles. *ISRN Nanotechnol*. 2012;2012:1-6.
12. Bhattacharyya S, Gedanken A. A template-free, sonochemical route to porous zno nano-disks. *Microporous Mesoporous Mater*. 2008;110(2-3):553-559.
13. Kumar R, Al-Dossary O, Kumar G, et al. Zinc oxide nanostructures for NO₂ gas-sensor applications: A review. *Nano-Micro Lett*. 2015;7(2):97-120.
14. Mitra P, Chatterjee AP, Maiti HS. Zno thin film sensor. *Mater Lett*. 1998;35(1-2):33-38.
15. Xu H, Liu X, Cui D, et al. A novel method for improving the performance of zno gas sensors. *Sensors Actuators, B Chem*. 2006;114(1):301-307.
16. Wang JX, Sun XW, Yang Y, et al. Hydrothermally grown oriented zno nanorod arrays for gas sensing applications. *Nanotechnology*. 2006;17(19):4995-4998.
17. Wang L, Kang Y, Liu X, et al. Zno nanorod gas sensor for ethanol detection. *Sensors Actuators, B Chem*. 2012;162(1):237-243.
18. Ong CB, Ng LY, Mohammad AW. A review of zno nanoparticles as solar photocatalysts: Synthesis, mechanisms and applications. *Renew Sustain Energy Rev*. 2018;81(August 2017):536-551.
19. Akhavan O. Graphene nanomesh by zno nanorod photocatalysts. *ACS Nano*. 2010;4(7):4174-4180.
20. Gonzalez-Valls I, Lira-Cantu M. Vertically-aligned nanostructures of zno for excitonic solar cells: A review. *Energy Environ Sci*. 2009;2(1):19-34.
21. Dvorak M, Wei SH, Wu Z. Origin of the variation of exciton binding energy in semiconductors. *Phys Rev Lett*. 2013;110(1):1-5.
22. Sun HD, Makino T, Segawa Y, et al. Enhancement of exciton binding energies in zno/znmgo multiquantum wells. *J Appl Phys*. 2002;91(3):1993-1997.
23. Gu Y, Kuskovsky IL, Yin M, et al. Quantum confinement in zno nanorods. *Appl Phys Lett*. 2004;85(17):3833-3835.
24. Ghosh R, Basak D, Fujihara S. Effect of substrate-induced strain on the structural, electrical, and optical properties of polycrystalline zno thin films. *J Appl Phys*. 2004;96(5):2689-2692.
25. Emanetoglu NW, Gorla C, Liu Y, et al. Epitaxial zno piezoelectric thin films for saw filters. *Mater Sci Semicond Process*. 1999;2(3):247-252.
26. Xu T, Wu G, Zhang G, et al. The compatibility of zno piezoelectric film with micromachining process. *Sensors Actuators, A Phys*. 2003;104(1):61-67.
27. Xie Y, He Y, Irwin PL, et al. Antibacterial activity and mechanism of action of zinc oxide nanoparticles against *Campylobacter jejuni*. *Appl Environ Microbiol*. 2011;77(7):2325-2331.
28. Kalpana D, Omkumar KS, Kumar SS, et al. A novel high power symmetric zno/carbon aerogel composite electrode for electrochemical supercapacitor. *Electrochim Acta*. 2006;52(3):1309-1315.
29. Yang P, Xiao X, Li Y, et al. Hydrogenated zno core-shell nanocables for flexible supercapacitors. *ACS Nano*. 2013;3(3):2617-2626.
30. Zhang L, Jiang Y, Ding Y, et al. Investigation into the antibacterial behaviour of suspensions of zno nanoparticles (zno nanofluids). *J Nanoparticle Res*. 2007;9(3):479-489.
31. Bai S, Wang L, Chen X, et al. Chemically exfoliated metallic mos₂ nanosheets: A promising supporting co-catalyst for enhancing the photocatalytic performance of tio₂ nanocrystals. *Nano Res*. 2014;8(1):175-183.

32. Tak Y, Yong K. Controlled growth of well-aligned zno nanorod array using a novel solution method. *J Phys Chem B*. 2005;109(41):19263-19269.
33. Park WI, Yi GC, Kim JW, et al. Schottky nanocontacts on zno nanorod arrays. *Appl Phys Lett*. 2003;82(24):4358-4360.
34. Goswami N, Sharma DK. Structural and optical properties of unannealed and annealed zno nanoparticles prepared by a chemical precipitation technique. *Phys E Low-Dimensional Syst Nanostructures*. 2010;42(5):1675-1682.
35. Pourrahimi AM, Liu D, Pallon LKH, et al. Water-based synthesis and cleaning methods for high purity zno nanoparticles-comparing acetate, chloride, sulphate and nitrate zinc salt precursors. *RSC Adv*. 2014;4(67):35568-35577.
36. M. Mazhdi, P. Hossein Khani. *Int.J.Nano Dim*. 2021;2(4): 233-240,
37. Bindu P, Thomas S. Estimation of lattice strain in zno nanoparticles: X-ray peak profile analysis. *J Theor Appl Phys*. 2014;8(4):123-134.
38. Sharmila PP, Tharayil NJ. DNA Assisted Synthesis, Characterization and Optical Properties of Zinc Oxide Nanoparticles. *Int J Mater Sci Eng*. Published online 2014:1-6.
39. Bhattacharjee CR, Purkayastha DD, Bhattacharjee S, et al. Homogeneous Chemical Precipitation Route to zno Nanosphericals. *Assam Univ J Sci Technol*. 2011;7(2):122-127.
40. Singh A, Vishwakarma HL. Study of structural, morphological, optical and electroluminescent properties of undoped zno nanorods grown by a simple chemical precipitation. *Mater Sci Pol*. 2015;33(4):751-759.
41. Yogamalar R, Srinivasan R, Vinu A, et al. X-ray peak broadening analysis in zno nanoparticles. *Solid State Commun*. 2009;149(43-44):1919-1923.
42. Kumar D, Kumar A, Prakash R, et al. X-ray Diffraction Analysis of Cu²⁺ Doped Zn_{1-x}Cu_xFe₂O₄ Spinel Nanoparticles using Williamson-Hall Plot Method. *AIP Conf Proc*. 2019;2142:4-8.
43. He HP, Zhuge F, Ye ZZ, et al. Strain and its effect on optical properties of Al-N codoped zno films. *J Appl Phys*. 2006;99(2).
44. Williamson GK, Smallman RE. III. Dislocation densities in some annealed and cold-worked metals from measurements on the x-ray debye-scherrer spectrum. *Philos Mag*. 1956;1(1):34-46.
45. Brus L. Electronic wave functions in semiconductor clusters: Experiment and theory. *J Phys Chem*. 1986;90(12):2555-2560.